Glu415 in the α-tubulins plays a key role in stabilizing the microtubule–ADP-kinesin complexes

Imre Gaspar* and Janos Szabad‡

University of Szeged, Faculty of Medicine, Department of Biology, Szeged, Hungary
*Present address: EMBL, Meyerhofstrasse 1, D-69117 Heidelberg, Germany
‡Author for correspondence (szabad@mdbio.szote.u-szeged.hu)

Accepted 16 April 2009
Journal of Cell Science 122, 2857-2865 Published by The Company of Biologists 2009
doi:10.1242/jcs.050252

Summary

***Kavar^{21g}*, a dominant female-sterile mutation of *Drosophila*, identifies the α*Tubulin67C* gene that encodes α4-tubulin, the maternally provided α-tubulin isoform. Although α4-tubulin is synthesized during oogenesis, its function is required only in the early cleavage embryos. However, once present in the developing oocyte, much of the α4-tubulin and the *Kavar^{21g}*-encoded E426K-α4-tubulin molecules become incorporated into the microtubules. We analyzed ooplasmic streaming and lipid-droplet transport, with confocal reflection microscopy, in the developing egg primordia in the presence and absence of α4-tubulin and E426K-α4-tubulin and learnt that the E426K-α4-tubulin molecules eliminate ooplasmic streaming and alter lipid-droplet transport. Apparently, Glu426 is involved in stabilization of the microtubule-kinesin complexes when the kinesins are in the most labile, ADP-bound state. Replacement of Glu426 by Lys results in frequent detachments of the kinesins from the microtubules leading to reduced transport efficiency and death of the embryos derived from the *Kavar^{21g}*-carrying females. Glu426 is a component of the twelfth α-helix, which is the landing and binding platform for the mechanoenzymes. Since the twelfth α-helix is highly conserved in the α-tubulin family, Glu415, which corresponds to Glu426 in the constitutively expressed α-tubulins, seems be a key component of microtubule-kinesin interaction and thus the microtubule-based transport.**

Supplementary material available online at
http://jcs.biologists.org/cgi/content/full/122/16/2857/DC1

Key words: α-tubulin, Microtubule-motor complex, Confocal reflection microscopy, Lipid-droplet transport, Ooplasmic streaming, *Drosophila melanogaster*

Introduction

Most of the factors required during early embryogenesis are maternally provided in the animal kingdom (DeRenzo and Seydoux, 2004; Tadros and Lipshitz, 2005). To understand some features of maternal effect, a set of dominant female sterile (Fs) mutations was induced and isolated in *Drosophila melanogaster* (Erdelyi and Szabad, 1989; Szabad et al., 1989). It was assumed that several of the Fs mutations identify genes that are engaged in the initiation and progression of embryogenesis. Elaborating their molecular functions may shed light on the beginning of new lives.

The *Tomaj^{D}* and the *Kavar^{D}* Fs mutations identify the α*Tubulin67C* gene (α*Tub67C*) (Mathe et al., 1998; Venkei et al., 2006; Venkei and Szabad, 2005), which encodes α4-tubulin, the so-called maternal α-tubulin, a rather divergent α-tubulin isoform (Kalfayan et al., 1982; Kalfayan and Wensink, 1982; Matthews et al., 1989; Matthews et al., 1993; Matthies et al., 1999; Theurkauf, 1992). (For a comprehensive list of the α4-tubulin-related references see FlyBase at http://flybase.bio.indiana.edu/.)

The α*Tub67C* gene is expressed during oogenesis in the nurse cells. The encoded α4-tubulin molecules are dumped into the egg cytoplasm and are utilized during early embryogenesis (Matthews et al., 1989; Venkei et al., 2006). They constitute about 20% of the α-tubulin pool in the *Drosophila* egg cytoplasm and their function cannot be replaced by the constitutively expressed α1-tubulin and α3-tubulin isoforms, products of the α*Tub84B* and α*Tub84D* genes (Matthews et al., 1989). Analysis of partial gain- and loss-of-function α*Tub67C* mutant alleles suggested the involvement of α4-tubulin in meiosis, cleavage mitoses, formation of the sperm aster and in the embryonic nervous system (Mathe et al., 1998; Matthews et al., 1993; Theurkauf, 1992; Matthies et al., 1999). Study of the mutant phenotypes associated with (1) *Kavar^{18c}*, one of the *Kavar^{D}* mutations, and (2) with the complete loss of α*Tub67C* gene function revealed that α4-tubulin is required for the fast formation of long microtubules (MTs) during the initial cleavage divisions (Venkei et al., 2006). The α4-tubulin molecules have been shown to be preferentially incorporated into the interpolar MTs and assist them in embracing the nuclear envelope. The interpolar MTs, which grow fast, push apart the daughter centrosomes along the nuclear perimeter to opposite poles in the early cleavage *Drosophila* embryos (Venkei et al., 2006).

Kavar^{21g}, another *Kavar^{D}* mutation, the result of a single base pair transition mutation (G1276→A), which causes the replacement of Glu426 by Lys [E426K-α4-tubulin (Venkei and Szabad, 2005)]. Glu426 resides in the twelfth α-helix of α4-tubulin, which – along with the eleventh α-helix and the unstructured C-terminus of the tubulin – is involved in formation of the outer surface of the MT lattice and has been implicated to be part of the landing and binding platform for the mechanoenzymes (Hoenger et al., 1998; Kikkawa and Hirokawa, 2006; Lakamper and Meyhofer, 2005; Mizuno et al., 2004; Wang and Sheetz, 2000). Mostly the positive residues of the kinesin head establish contact with the negatively charged MT surface in the landing and binding platform (Marx et al., 2006; Woehlke et al., 1997). Some of the negatively charged amino acids in the twelfth α-helix of the β-tubulins (E410, D417, E421) have been shown to be necessary to sustain the microtubule-kinesin interaction in the ATP-bound strong binding state (Uchimura et al., 2006). Removal of the C-terminus of the tubulins (by subtilisin digestion) decreases the processivity and the transport efficiency

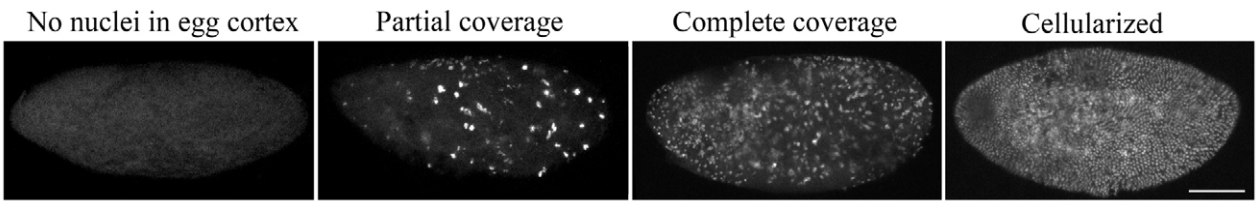

Fig. 1. The presence and the coverage of the egg cortex by nuclei in different types of embryos derive from the *Kavar*^{21g}/+ females. The wild-type embryos appear very similar to the 'cellularized' embryo. Scale bar: 100 μm.

of the associated mechanoenzymes through the regulation of the rate of ADP release and the transition to the next duty cycle of the motor head (Lakamper and Meyhofer, 2005; Wang and Sheetz, 2000).

To understand the mode of E426K-α4-tubulin action and the basis of the *Kavar*^{21g}-related sterility, we analyzed ooplasmic streaming and the kinetics of lipid-droplet transport, using confocal reflection microscopy (CRM), in developing *Drosophila* egg primordia (Gaspar and Szabad, 2009). We report here that replacement of Glu426 by Lys in α4-tubulin brings about (1) a complete cessation of the fast ooplasmic streaming in the developing oocyte and (2) a decrease in lipid-droplet transport efficiency. E426K-α4-tubulin reduces the average transport speed and the dwell time, and consequently results in shorter than normal runs of the cargo. The E426K-α4-tubulin-related defects stem most probably from a decreased stability of the MT-kinesin complexes and are related to the impaired stabilizing forces in the ADP-bound state of the motor head, as has also been suggested by molecule models (Kikkawa and Hirokawa, 2006; Yonekura et al., 2006). The importance of Glu426 in the MT-kinesin interaction is strongly supported by the genetic interaction between *Kavar*^{21g} and loss-of-function mutant alleles of the different kinesin family members.

Since (1) the twelfth α-helix of α4-tubulin, containing Glu426, is highly conserved within all the 42 known α-tubulin isoforms in 32 species analyzed (in a BLAST analysis), (2) Glu426 in α4-tubulin corresponds to Glu415 in the evolutionary highly conserved α-tubulins, and (3) Glu415 is 100% conserved evolutionarily in all the studied α-tubulin isoforms, we propose that Glu415 plays a key role in stabilizing the microtubule–ADP-kinesin complexes.

The approach presented in this paper may be of special importance since the replacement of Glu415 by Lys in the evolutionarily highly conserved and constitutively expressed α-tubulins is expected to bring about dominant lethality. However, the same types of mutations in the α4-tubulin encoding α*Tub67C* gene alter fate of only the egg primordia and the descending embryos and do not affect viability of the adults. The developing egg primordia thus offer a convenient system to analyze the mutation-related defects and provide a profound understanding about the roles of the different amino acids in the MT-associated functions.

Results

The *Kavar*^{21g}-encoded E426K-α4-tubulin inhibits ooplasmic streaming

Embryogenesis does not commence or proceeds abnormally inside the otherwise normal looking eggs of the *Kavar*^{21g}/+ females: several of the cleavage nuclei fail to migrate into the egg cortex leaving large areas free of nuclei (Fig. 1) (Venkei and Szabad, 2005). The *Kavar*^{21g}-related defects presumably arise from altered abilities of the MTs to function as migration routes for the motor molecules since the *Kavar*^{21g}-encoded E426K-α4-tubulin molecules do not prevent microtubule formation (Venkei and Szabad, 2005) (see also Fig. 4). In fact, cleavage spindles do form in embryos of the *Kavar*^{21g}-carrying females (see supplementary material Movies 1

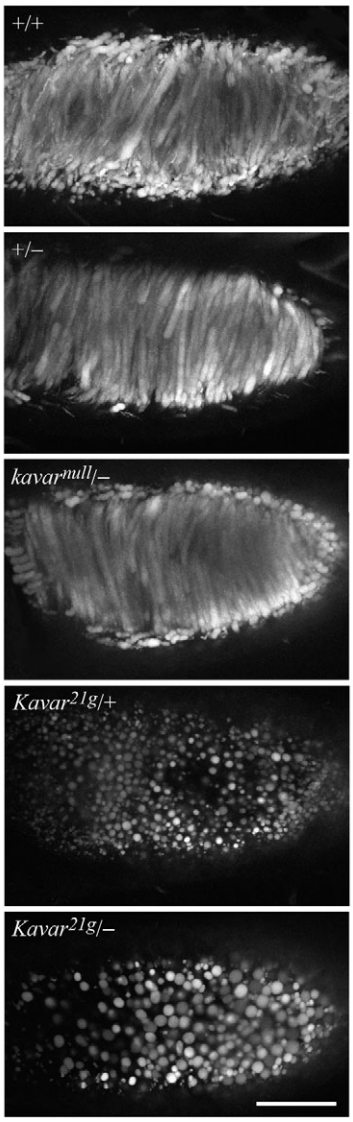

Fig. 2. Ooplasmic streaming in the stage 11 oocytes. Yolk autofluorescence was imaged on 50 successive frames representing 3 minutes. The images were combined to produce streak projections. There is no ooplasmic streaming in presence of the *Kavar*^{21g}-encoded E426K-α4-tubulin, i.e. in oocytes of the *Kavar*^{21g}/+ and the *Kavar*^{21g}/– females. Ooplasmic streaming appears normal in the absence of α4-tubulin, i.e. in oocytes of the *kavar*^{null}/– females. Scale bar: 50 μm.

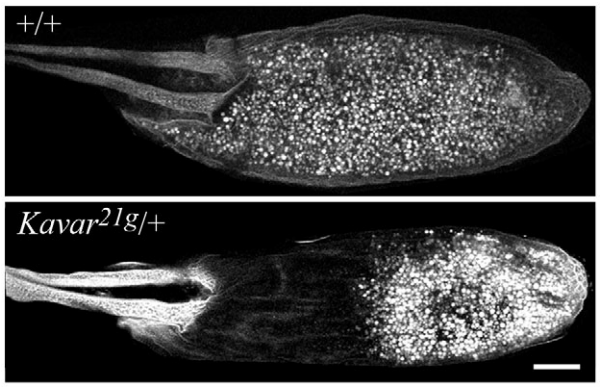

Fig. 3. In the absence of ooplasmic streaming the follicle-cell-produced yolk granules accumulate in the posterior egg cytoplasm in the stage 14 oocytes (also in eggs) of the *Kavar*^{21g}-carrying females. However, the posterior accumulation of the yolk granules does not led to the failure of embryogenesis (Serbus et al., 2005). Scale bar: 50 µm.

and 2), although they are frequently abnormal. Because embryogenesis in eggs laid by *Kavar*^{21g}-carrying females suffers from a wide range of defects, we decided to analyze the developing late egg primordia to elucidate the mode of E426K-α4-tubulin action. As several components of the egg cytoplasm are transported along the MTs in the growing oocyte during oogenesis, we decided to study two transport processes in the developing egg primordia, (1) ooplasmic streaming and (2) transport of the lipid droplets.

During ooplasmic streaming the entire ooplasm swirls around the longitudinal axis of the egg primordia to ensure the mixing of the yolk-free cytoplasm (dumped from nurse cells into the oocyte) with the follicle-cell-derived yolk granules. The process is propelled mostly, if not exclusively, by kinesin heavy chain (KHC) in the stage 10B-12 oocytes (Palacios and St Johnston, 2002; Serbus et al., 2005) (Fig. 2). Although the yolk granules stream steadily along a linear paths at about 350 nm/second in the control oocytes [362±5 nm/second in the wild type (+/+) and 348±5 nm/second in the heterozygous (+/–) oocytes; mean ± standard error of the mean), there is no ooplasmic streaming in presence of E426K-α4-tubulin, that is in the egg primordia of the *Kavar*^{21g}/+ and the *Kavar*^{21g}/– hemizygous females (Fig. 2; '–' stands for *Df(3L)55*, a short deficiency that removes the α*Tub67C* and three of the adjacent genes) (Venkei and Szabad, 2005). The absence of ooplasmic streaming leads to a gradual accumulation of the yolk granules in the posterior oocyte cytoplasm, thus leaving the anterior cytoplasm free from the yolk granules (Fig. 3). A plausible explanation for the lack of ooplasmic streaming could be an absence of the sufficiently long MTs in the oocytes, as was reported for the egg primordia of the *Kavar*^{18c}-carrying females (Venkei et al., 2006). The *Kavar*^{18c}-encoded E82K-α4-tubulin molecules become incorporated into the MTs and prevent the formation of sufficiently long MTs, which are required for ooplasmic streaming (Venkei et al., 2006; Gaspar and Szabad, 2009). In contrast to the *Kavar*^{18c}-carrying egg primordia, there are numerous and long MTs present in oocytes containing the E426K-α4-tubulin at stages 10B-12, as revealed by the distribution of Jupiter-GFP highlighted MTs (Fig. 4). However, and unlike in the wild-type oocytes, the MTs of these oocytes do not form thick parallel bundles, most probably as a consequence of the abnormal MT-kinesin interaction.

Remarkably, there is ooplasmic streaming in egg primordia of the *kavar*^{null}/– females, i.e. in the absence of α4-tubulin, although

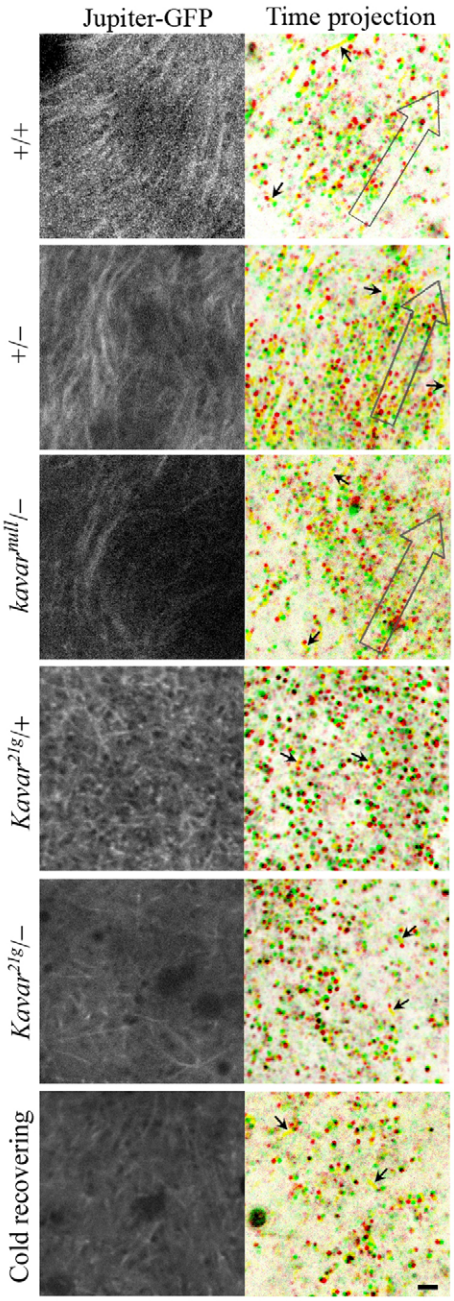

Fig. 4. MT organization and lipid-droplet motion in the early stage 12 oocytes. The time projection images were prepared by projecting 100 successive reflection images in 6.5 seconds at 633 nm. The beginnings of the paths appear red, followed by yellow and finish up in green. The non-moving particles appear black. The MT images were prepared by taking the average of the middle ten (in the presence of streaming) or all the frames (in the absence of streaming) of the GFP channel of the corresponding time-lapse recording. In the wild-type (+/+), in the hemizygous (+/–) and in the α4-tubulin (–/–)-lacking early stage 12 oocytes a large proportion of the lipid droplets flow by the streaming ooplasm parallel with the majority of the MTs (open arrows). In addition to these lipid droplets, there is a subset of lipid droplets that move independently of streaming (arrows). Note that there are many and long MTs in the oocyte cytoplasm in the presence of E426K-α4-tubulin (in the *Kavar*^{21g}/+ and the *Kavar*^{21g}/– females). However, these MTs are not organized into parallel bundles as in wild type. The MTs are also disorganized in the wild-type oocytes during the recovery from cold treatment. Although there is no streaming in the E426K-α4-tubulin-containing and in the cold-treated egg primordia, some of the lipid droplets are transported along linear paths, along the MTs (arrows). Scale bar: 2 µm.

Table 1. Features of the genetic interaction between *Kavar^{21g}* and the kinesin encoding genes

	Embryo	Nuclear coverage of the egg cortex (%)†				P‡
		None	Partial	Complete	Cellularized	
+/+ Controls						
+/+	228	6.6	0.4	0	93.0	–
khc^{8}/+	527	9.5	0	0	90.5	0.509
Df(3L)ED202/+	254	9.1	0	0	90.9	0.314
cand/+	529	2.8	0	0	97.2	0.614
Dhc64C$^{4-16}$/+	1176	8.3	0	0	91.7	0.784
Gl^{1}/+	160	3.8	0	0	96.3	0.514
***Kavar^{21g}*/+**						
+/+	343	55.1	16.6	28.0	0.3	–
khc^{8}/+	156	75.0	6.4	16.7	1.9	<0.001*
Df(3L)ED202/+	126	76.2	11.9	11.9	0	<0.001*
cand/+	215	47.9	8.8	43.3	0	0.002*
Dhc64C$^{4-16}$/+	155	58.7	14.8	25.8	0.6	0.761
Gl^{1}/+	216	65.3	7.4	27.3	0	0.030

†Percentage of the different types of 3- to 4-hour-old embryos. None, no nuclei in the egg cortex; partial, the nuclei populate some part of the egg cortex; complete, although nuclei populate the egg cortex, cells do not form or only very few cells form; cellularized, embryos resemble the normal cellular blastoderm (see also Fig. 1).

‡P-value of the χ^2 tests against the corresponding control group, i.e. those +/+ or *Kavar^{21g}*/+ females that carried two copies of the motor encoding genes.

*Significant differences.

The *Df(3L)ED202* deficiency uncovers the *Klp61F* locus.

the average streaming velocity of the yolk granules drops from 348±5 to 317±8 nm/second (P<0.001, as compared with the +/– control; Fig. 2). This observation indicates that α4-tubulin is not required for ooplasmic streaming, although its presence influences the process. The E426K-α4-tubulin-related defects originate from the direct effect of the mutant E426K-α4-tubulin molecules and not from the absence of α4-tubulin function, thus excluding the dominant negative nature of *Kavar^{21g}*.

The genetic interaction between *Kavar^{21g}* and the kinesin genes indicates altered MT-based transport

The *Kavar^{21g}*-associated mutant phenotypes and position of the Glu426→Lys replacement suggested altered interaction between MTs and mechanoenzymes and MT-based transport in the presence of E426K-α4-tubulin. To test this possibility, we constructed *Kavar^{21g}*/+ females from which one copy of a motor-encoding gene was removed (either by a mutation or by a deficiency; Table 1). We then analyzed 3- to 4-hour-old embryos and determined how far they had progressed in development (as illustrated in Fig. 1). The results are summarized in Table 1 and clearly show a genetic interaction between *Kavar^{21g}* and the studied members of the kinesin gene family. Upon removal of one copy of the genes encoding the plus end tracking motor kinesin heavy chain *khc* or the bipolar kinesin *klp61F* from *Kavar^{21g}*/+ flies, the early cleavage defects occur in a significantly larger proportion of embryos than in embryos of the control *Kavar^{21g}*/+ females (Table 1). Upon removal of one copy of the *ncd* gene, which encodes the *Drosophila* minus-end kinesin, the embryos reach a later stage in development than the control embryos (Table 1). In contrast to the kinesins, the removal of one copy of *Dhc64C* (which encodes cytoplasmic dynein heavy chain) or the *Glued* (which encodes a major subunit of the dynein regulator dynactin) did not alter the *Kavar^{21g}*-imposed defects, implying that E426K-α4-tubulin does not perceptibly affect the dynein-based transport (Table 1). (Note that the removal of one cope of any of the studied MT-motor encoding genes does not reduce the viability of the embryos from females with two normal α*Tub67C* genes; Table 1.) The genetic interaction between *Kavar^{21g}* and the kinesins suggests an important role of Glu426 in α4-tubulin in the MT-kinesin interaction and therefore in MT-based transport.

Table 2. Parameters of lipid-droplet transport in the early stage 12 *Drosophila* egg primordia

Genotype or treatment	Egg primordia analyzed	Lipid droplets		Number of runs	Average speed§ (nm/s)	P¶	Run length§ (nm)	P††	Run time§ (ms)	P††
		Density‡	Droplets analyzed							
+/+	10	15.4±1.2	309	405	908±15	–	1033±41	–	1178±47	–
+/–	8	22.9±3.0	393	477	917±14	0.990	1083±54	0.493	1222±41	0.722
kavar^{null}/–	8	18.4±5.0	294	380	763±12	<0.001*	898±40	0.049	1209±51	0.635
Kavar^{21g}/+	6	15.1±3.1	182	215	757±21	<0.001*	550±28	<0.001*	792±41	<0.001*
Kavar^{21g} /–	6	17.3±5.6	208	259	743±18	<0.001*	647±31	<0.001*	940±48	<0.001*
+/+; cold recovering†	5	13.9±1.9	139	171	866±25	0.406	1034±52	0.992	1257±64	0.389

†Five minutes before complete recovery of ooplasmic streaming. The complete recovery of ooplasmic streaming usually takes 15 minutes (Gaspar and Szabad, 2009).

‡The number of motile lipid droplets that appeared during recording over a 20.9×20.9 μm^2 cytoplasm area in a 19.5 second recording period. Means ± s.e.m.

§Means ± s.e.m.

¶P-value of Dunnet's post-hoc multiple comparison of the mean velocity in one-way ANOVA using wild type (+/+) as control.

††P-value of survival curve comparison with Cox regression using wild type (+/+) as control.

*Significantly different from the corresponding (+/+) control.

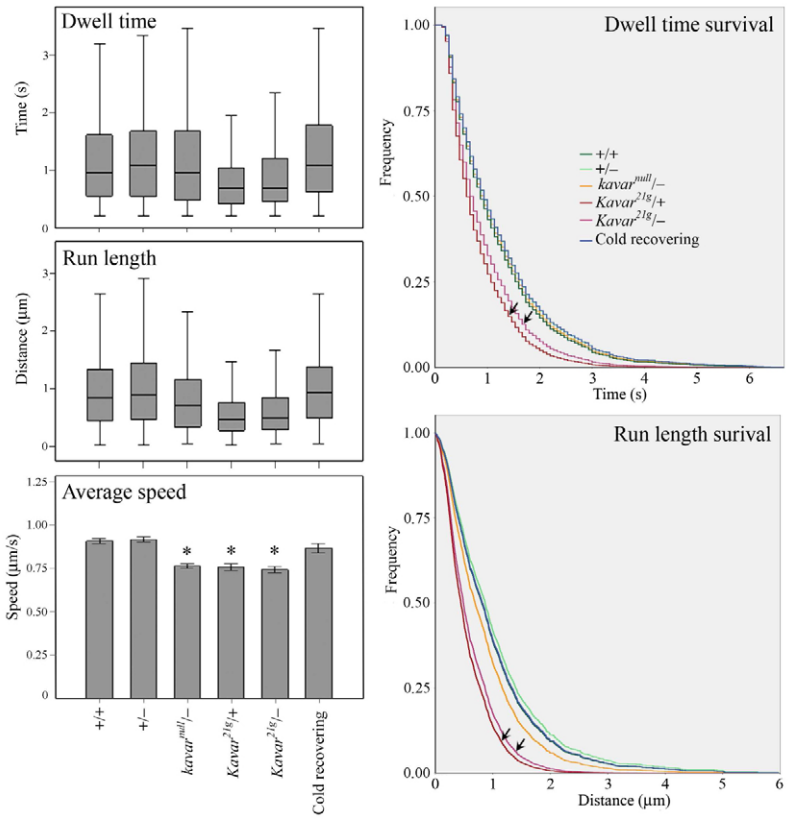

Fig. 5. Motion parameters of lipid-droplet transport. In the presence of the *Kavar*^{21g}-encoded E426K-α4-tubulin, both the dwell time and the run length decrease (box plots; the 10th, 25th, 50th, 75th and 90th percentiles are represented). There is also a small, but significant reduction in the speed of motion (means ± s.e.m.; *P<0.001). The absence of α4-tubulin does not lead to a significant change in run time and run length, although it results in a similar decrease in the average speed of motion as seen in the presence of E426K-α4-tubulin. The dwell time and the run lengths were compared by survival analyses. E426K-α4-tubulin causes significant reduction in the time available for motion and thus in the effective range of the transport (as compared with the wild type, +/+; P<0.005 for both *Kavar*^{21g}/+ and *Kavar*^{21g}/–; arrows). 'Cold recovering' is a type of control, where ooplasmic streaming was eliminated by cold treatment. The analysis was conducted during a subsequent 10 minute 'warming up' time, 5 minutes before the ooplasmic streaming resumed.

E426K-α4-tubulin interferes with MT-mediated lipid-droplet transport

The complete blockage of ooplasmic streaming in the presence of E426K-α4-tubulin indicates severe difficulties in MT-motor interaction. To characterize the nature of the E426K-α4-tubulin-related defects, we studied transport of the ~0.5 μm lipid droplets in the ooplasm of the developing egg primordia. The lipid droplets, which are dumped in high numbers into the oocyte cytoplasm from the nurse cells during oogenesis, are not only the mayor lipid storage vesicles but are sites of protein sequestration and appear to be engaged in regulated inactivation of proteins, preventing the formation of toxic protein aggregates and delivery of signalling molecules (Welte, 2007). The lipid droplets have been known to be transported along the MTs by the mechanoenzymes during oogenesis and embryogenesis (Welte et al., 1998; Gross et al., 2000; Shubeita et al., 2008; Gaspar and Szabad, 2009). The refractive nature of the lipid droplets offers a convenient way, using CRM, to study their motion in the oocyte cytoplasm of the developing egg primordia (Paddock, 2002; Vesely and Boyde, 2001; Gaspar and Szabad, 2009).

Surprisingly, although E426K-α4-tubulin completely abolishes ooplasmic streaming, it does not inhibit the motion of those lipid droplets that move independently of streaming through the MT-based active transport mechanism (Fig. 4) (Gaspar and Szabad, 2009). Although the plus- and the minus-end-directed motions cannot be distinguished in the absence of ooplasmic streaming, analysis of the moving lipid droplets may well reveal the effects of E426K-α4-tubulin on MT-based transport. With this idea in mind, we focused attention on lipid-droplet motion in the ooplasm of the early stage 12 egg primordia. Considering the possible modifying effects of the viscous load that may be exerted by the flowing ooplasm on the transported lipid droplets, we analyzed wild-type, early stage 12 oocytes that were in the process of recovering from cold treatment. Note that ooplasmic streaming, as all the MT-based transports, cease upon cold treatment as a result of depolymerization of the MTs. MTs form again during the recovery from clod treatment and although the lipid-droplet transport along the MTs resumes, ooplasmic streaming is still absent during the subsequent 12-15 minutes (Gaspar and Szabad, 2009).

Although the number of the motile lipid droplets is similar over the studied cytoplasmic region and during the recording time in the egg primordia of the females with different genotype (as listed in Table 2), the average velocity of the lipid droplets is significantly lower in the presence of E426K-α4-tubulin as compared with the control (Table 2, Fig. 5). Moreover, the average dwell time and thus the run lengths decrease in the presence of E426K-α4-tubulin (Table 2). The average run length, i.e. the effective transport range of a single run, drops to 60% of wild-type run length (Table 2). To test the significance of the decrease in dwell time and run lengths in the presence of E426K-α4-tubulin, we carried out survival analyses of these parameters, i.e. we tested the survival rate of the lipid droplet runs as a function of time and distance travelled. Apparently, the dwell time and consequently the run length are significantly shorter in the presence of E426K-α4-tubulin than in the control oocytes (Table 2, Fig. 5).

Absence of α4-tubulin also results in significant decrease in the speed of the lipid droplets, as in the presence of E426K-α4-tubulin. This finding may cast doubt on the independent action of E426K-α4-tubulin from the α4-tubulin function. However, the survival analyses of both the dwell time and the run length revealed no significant departure from the wild-type control values (Table 2, Fig. 5). The dwell time findings indicate that although the presence

Table 3. Duration and frequencies of the different events that follow the ending of lipid droplet runs

		Pauses‡			Track switches‡				Stuck‡	
Genotype or treatment	Track	Number	%	Duration (ms)¶	Number	%	Duration (ms)¶	P§	Number	%
+/+	405	84	20.7	184±10	15	3.7	217±34	–	0	0
+/–	477	65	13.6	196±15	29	6.0	419±77	0.249	2	0.4
kavar^{null}/–	380	72	18.9	161±9	27	7.1	510±101	0.346	1	0.3
Kavar^{21g}/+	215	33	15.3	213±22	10	4.7	130±14	0.715	3	1.4
Kavar^{21g}/–	259	40	15.4	187±13	20	7.7	390±98	0.141	2	0.8
+/+; cold recovering†	405	25	14.6	167±14	12	7.0	580±164	0.172	0	0

†Five minutes before complete recovery of ooplasmic streaming.

‡Pause types in lipid droplet motion. During pauses, the lipid droplet idles and then resumes motion in the same direction as before. During track switches the lipid droplet stops and starts motion again in a statistically different direction. During stuck the cargo does not move away (cf. Gaspar and Szabad, 2009).

§Probability values of χ^2 tests comparing the frequencies of pauses and track switches to those in the wild type (+/+) control. (The stuck events were omitted from the test because of low numbers.)

¶Means ± s.e.m.

of α4-tubulin in the MTs may increase motor processivity through velocity, i.e. the number of steps taken by the motor during a period, it has no significant influence on the dwell time of the travelling motor by altering the MT-motor dissociation rate, or by some other way. It can thus be deduced that the absence of the α4-tubulin molecules has no significant impact on the effective range of the single runs.

Apparently, the basis of the deleterious action of E426K-α4-tubulin is a reduced effective range of transport runs. However, it is not clear how E426K-α4-tubulin disturbs the transport along the MTs. Does it increase the MT-motor dissociation rate or does it bring the motor head into a rigorous state by trapping the cargo, as was described for E164A-KHC (Klumpp et al., 2003)? Analysis of the ends of the single runs revealed three types of events: (1) The lipid droplets dissociate from the track and diffuse away in about 80% of cases. Some of the droplets regain motion after a short pause. These droplets move away either (2) by using the same track (~15%) or (3) by changing track (~5%, i.e. there is a significant change in the direction of the motion). The average time is about 0.5 seconds in changing track and is about 0.2 seconds for in the 'track-keeping' pauses. The parameters of the ending events did not change significantly in the presence of E426K-α4-tubulin, implying that the trapping hypothesis is more than unlikely (Table 3).

A fraction of the dissociating lipid droplets could be followed for more than two frame intervals after the ending event (0.195 seconds). A mean square displacement (MSD) analysis of these lipid droplets revealed that E426K-α4-tubulin does not influence the free diffusion of the lipid droplets, which otherwise followed a more-or-less linear path after they dissociated from MTs (Fig. 6). The frequency of the trapped lipid droplets that finished their motion with a pause (stuck), remained very low irrespective of the presence or absence of E426K-α4-tubulin (Table 3). The present findings exclude the possibility of the trapping mode of E426K-α4-tubulin action.

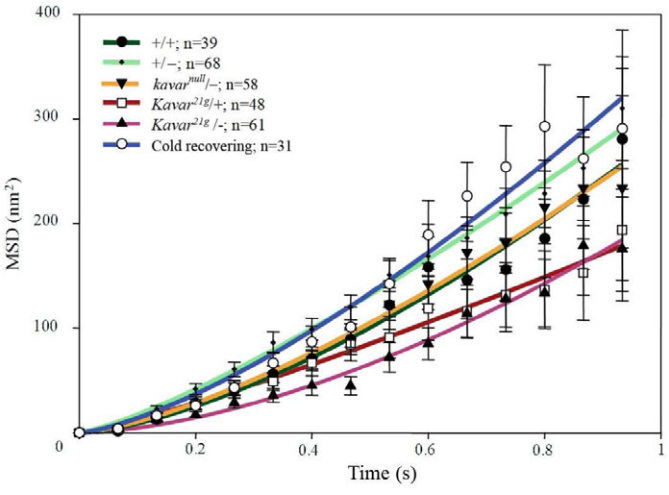

Fig. 6. Mean square displacement (MSD) of lipid droplets after finishing their linear runs. Motion of lipid droplets that could be followed for at least three frame intervals after strict linear displacements, were analyzed and fitted by quadratic functions with r^2>0.95 each. MSD of the lipid droplets follows quadratic curves and does not reach saturation in the presence of E426K-α4-tubulin, indicating no motion-limiting events (i.e. stuck) at the end of the runs. The data are means ± s.e.m.

Discussion

To ship a wide variety of components, the eukaryotic cells rely largely on the MTs and the associated transport mechanisms. In *Drosophila*, as in many other animal species, the MT-based machinery is especially important during early embryogenesis when the cleavage cycles are repeated every 8-10 minutes and the MTs need to span over large distances (Foe et al., 1993; Tadros and Lipshitz, 2005). In fact, α4-tubulin, a special α-tubulin isoform could be said to be 'designed' to meet the unusual requirements associated with the MTs during the early cleavage divisions (Venkei et al., 2006). Although the overall homology is only about 70% between α4-tubulin and the evolutionarily highly conserved members of the α-tubulin family, the C-terminal structures, especially the twelfth α-helix, show 96% homology to other members of the α-tubulin family (Fig. 7). This region of the α-

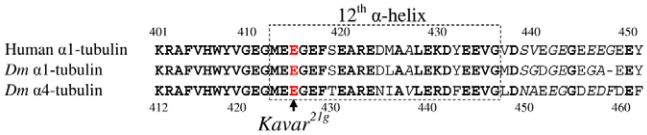

Fig. 7. The twelfth α-helix of the α-tubulins is highly conserved. Although α4-tubulin is a divergent member of the α-tubulin family, the twelfth α-helix posses 88% identity and 100% homology with other family members, suggesting a general role of the E426 α4-tubulin residue in MT-related function. Identical amino acids are in bold, similar amino acids are in normal type and different ones in italic type. E is replaced by K in the *Kavar*^{21g}-encoded mutant α4-tubulin.

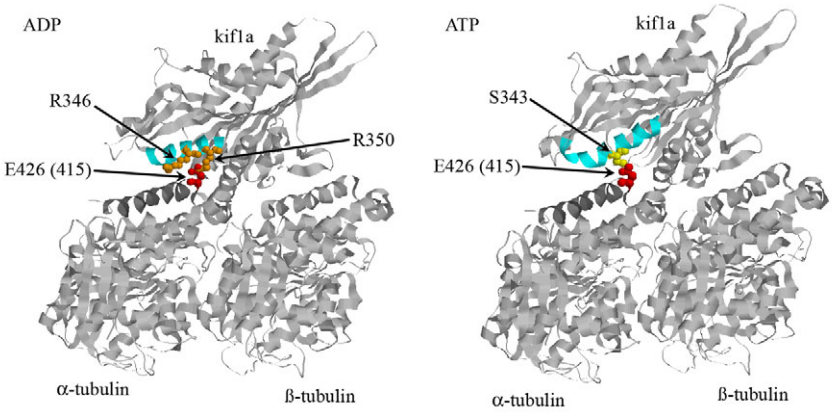

Fig. 8. Model to explain the mode of E426K-α4-tubulin action. Glu426 (which corresponds to Glu415 in other members of the α-tubulin family) is in close proximity to two positively charged arginine residues (Arg346 and Arg350) that reside in the head domain of kif1a, a kinesin family member, when the motor binds to ADP (see PDB-ID: 2HXH (Kikkawa and Hirokawa, 2006). The forming ionic bonds are thought to play a key role in binding the motor to the MT surface during this otherwise weakly bound state. (Naturally, the involvement of the nearby amino acid residues cannot be ruled out in ensuring the MT-motor contact.) Replacement of Glu426 by lysine reverses the binding force, which leads to weaker-than-normal MT-motor interaction in the ADP-bound state of the motor and thus frequent MT-motor dissociations and reduced transport efficiency. Glu426 well may also participate in stabilizing the ATP bound head to the MTs by establishing interactions with the nearby Ser343 residue (see PDB-ID: 2HXF) (Kikkawa and Hirokawa, 2006). The molecular models were prepared using RasMol (http://www.umass.edu/microbio/rasmol/getras.htm).

tubulins participates in forming the outer surface of the MTs, where most of the MT-protein interactions take place, including landing and binding of the mechanoenzymes (Marx et al., 2006). Since the *Kavar*^{21g} mutation resulted in a Glu→Lys replacement in the position 426, which is a component of the twelfth α-helix, a disturbed MT-mechanoenzyme interaction may well account for the *Kavar*^{21g}-related defects.

Indeed, the genetic interaction between *Kavar*^{21g} and members of the kinesin family genes clearly confirmed the above assumption and showed an involvement of Glu426 in interactions with (1) KHC, the major component of the classical kinesins that is involved in several MT-dependent transport processes (Saxton et al., 1991); (2) the mitotic kinesin Klp61F, the orthologue of Eg5, a bipolar kinesin that provides the force necessary to keep the mitotic spindle bipolar and acts against the spindle contractor motor; and (3) NCD, a minus-end-directed kinesin. In wild-type embryos, the poleward and plateward forces exerted by Klp61F and NCD are in a strict spatiotemporal balance in maintaining spindle integrity during the cell cycles (Cytrynbaum et al., 2003; Sharp et al., 2000). E426K-α4-tubulin appears to bring about a disturbance in the coordination of the kinesin motors as indicated by the high divergence in the size and shape of the cleavage spindles and by the consequent loss of many of the cleavage nuclei in embryos of the *Kavar*^{21g}-carrying females (Venkei and Szabad, 2005). Although a partial removal of Klp61F brings about a shift in the already unbalanced spindles toward spindle collapses, partial removal of *ncd*, increases the frequency of the seemingly normal divisions. Although it is not clear how removal of one copy of the KHC encoding gene brings about earlier-than-usual arrest of embryogenesis of the *Kavar*^{21g}/+-derived embryos, the involvement of KHC in embryogenesis has already been shown (Serbus et al., 2005).

To understand the mode of E426K-α4-tubulin action and the role of Glu426 in MT-kinesin interaction, we made use of the fact that α4-tubulin is not essential for the formation of normal eggs and is used only during the initial cleavage divisions (Venkei et al., 2006) (and this paper). However, once produced in the nurse cells and dumped into the oocyte cytoplasm from stage 10 of egg primordia development, much of the α4-tubulin and the E426K-α4-tubulin molecules are incorporated into the MTs and thus provide a convenient means of analysis of the role of Glu426 in MT-kinesin interaction. The egg primordia develop normally in the *Kavar*^{21g}/+ females and the MT-based transport processes are not hampered by E426K-α4-tubulin up to stage 10, the time when the amount of α4-tubulin starts to increasing in the ooplasm. Simultaneously, the MT-based transport processes become pronounced in the oocyte. In the presence of E426K-α4-tubulin the fast ooplasmic streaming is absent as it happens following the removal of KHC from the ooplasm (Serbus et al., 2005). Since absence of the wild-type α4-tubulin has little impact on the process, it is safe to conclude that E426K-α4-tubulin is responsible for the stoppage of ooplasmic streaming. E426K-α4-tubulin most probably acts through interfering with KHC, the stream-propelling motor, and not by blocking wild-type α4-tubulin function.

As revealed by analysis of lipid-droplet transport, E426K-α4-tubulin disrupts MT-based transport through decreasing the effective transport range of the carrier-cargo complexes. The basis of E426K-α4-tubulin action is almost certainly an increase in the MT-motor dissociation rate. During the duty cycle, the two-headed kinesin molecules effectively couple the chemical energy release from ATP to mechanical force exertion (Schief and Howard, 2001). In this process not only those structures that are engaged in binding the motor head domain change over the MT surface, but also the binding force is altered along with a change in the nucleotide state of the motor (Cross, 2004). The MT-motor complex reaches the most labile state during the release of ADP from the leading head (Schief et al., 2004). The speed of ADP release is relatively slow compared with the detachment rate of the trailing head, and there is an approximately 1% chance, even under normal conditions, for dissociation of the MT-motor complex (Schief et al., 2004). An assessment of the MT-kinesin head complex revealed two positively charged Arg residues in the sixth α-helix of the ADP-bound kinesin head domain residing in close vicinity of Glu426 (Fig. 8) (Kikkawa and Hirokawa, 2006). It is probable that the ionic interaction between these three amino acids is responsible for the stabilization

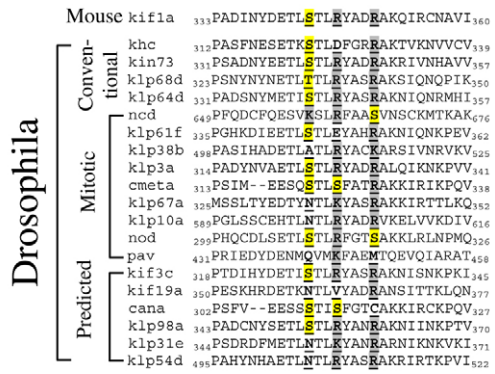

Fig. 9. The residues that interact with Glu426 of α4-tubulin are well conserved in members of the kinesin family. The positively charged arginine residues are highlighted in grey. The amino acid residues that can form hydrogen bonds with Glu426 are highlighted in yellow.

of the motor head on the MT during this labile state (Yun et al., 2003; Yonekura et al., 2006), although it cannot be ruled out that E426K-α4-tubulin may alter the overall structure of the twelfth α-helix, and thus the destabilization of the MT-kinesin complexes may be the consequence of several altered residue-residue interactions.

In support of the former hypothesis, an analysis of the homologous region in members of the *Drosophila* kinesin family revealed that the two positively charged residues, especially the second one, are well conserved in the kinesin motors (Fig. 9). The charge reversal imposed by the E426K-α4-tubulin molecules reduces or abolishes the binding force and thus increase the instability of the MT-kinesin complex, leading to frequent MT-motor dissociations. Knowing that α4-tubulin comprises about 20% of the α-tubulin pool in the egg cytoplasm (Matthews et al., 1989), E426K-α4-tubulin is present in about 10% of the tubulin heterodimers in the MTs, posing possible sites for kinesin drop offs and thus reduced transport efficiency. Since many of the kinesin motors carry on various functions during the cleavage mitoses, it is understandable how *Kavar*^{21g} can bring about a wide range of defects that lead to female sterility.

The *Kavar*^{21g}-related Glu426→Lys amino acid exchange came about in the twelfth α-helix, in a region that is highly conserved in other members of the α-tubulin family (Fig. 7). Since Glu426 corresponds to Glu415 in the constitutively expressed α-tubulin isoforms and Glu415 is evolutionary 100% conserved in every member of the α-tubulin family, it appears that Glu415 plays a key role in stabilization of the ADP-kinesin head on the MT surface and is thus a key component of the MT- and kinesin-based transport.

Owing to the highly conservative nature and crucial functions of the MTs in all the eukaryotic cell types, a mutation producing a Glu415→Lys change in the constitutively expressed *Drosophila* α1- or in the α3-tubulin would presumably bring about dominant lethality and make analysis of the role of the studied amino acids practically impossible. However, such mutations could be of great help in understanding the motor-interacting properties and other surface-associated MT functions. Expression of the α*Tub67C* gene during development of the egg primordia offers a convenient analysis of the encoded mutant proteins in MT-based transport and an elucidation of the role of any particular residues of the α(4)-tubulins in the process.

Materials and Methods

Fly stocks

Kavar^{21g} is a dominant female-sterile mutation in the α*Tub67C* gene of *Drosophila melanogaster* and encodes E426K-α4-tubulin (Erdelyi and Szabad, 1989; Venkei and Szabad, 2005). X-ray-induced reversion of *Kavar*^{21g} resulted in the formation of *kavar*^{rX21} (designated as *kavar*^{null}), a complete loss-of-function allele of the α*Tub67C* gene (Venkei and Szabad, 2005).

To conduct the genetic interaction tests, we generated *Kavar*^{21g}/+ (and, as control, +/+) females from which one copy of either of the following MT-motor-encoding genes were removed by a mutation or by a short deficiency: (1) *kinesin heavy chain* by *khc*^{8}, a null allele (Saxton et al., 1991), (2) *klp61F* by the *Df(3L)ED202* deficiency, (3) *non-claret-disjunctional* (*ncd*$^{-}$) by *Df(3R)ca*nd (Yamamoto et al., 1989), (4) *cytoplasmic dynein heavy chain* by *Dhc64C*$^{4-16}$, a hypomorphic mutant allele (Gepner et al., 1996) and (5) *Glued*, a mayor component of the dynactin complex, by the null allele *Gl* (Ghosh-Roy et al., 2004). For an explanation of the genetic symbols see FlyBase at http://flybase.bio.indiana.edu.

To label the MTs, a *Jupiter-GFP* expressing transgenic line was used (Karpova et al., 2006). *Jupiter-GFP* and *Df(3L)55* were recombined onto the same chromosome. The *Jupiter-GFP Df(3L)55/Kavar*^{21g} females were descended from a cross between *Jupiter-GFP Df(3L)55/TM3, Sb Ser* females and *Kavar*^{21g}*/TM3, Sb Ser* males. The flies were raised on standard food and kept on 25°C.

Embryo collection and staining

Three- to four-hour old embryos were collected from females of different genotypes (as listed in Table 1). The embryos were fixed as described by Venkei et al. (Venkei et al., 2006), stained with 1 μg/ml Hoechst 33342 (Sigma 14533) for 15 minutes. The embryos were then scored for nuclear phenotype (Fig. 1).

In vivo imaging of the egg primordia

Ovaries were dissected and the egg primordia were prepared for analysis as described by Gaspar and Szabad (Gaspar and Szabad, 2009). Briefly, the ovarioles were dissected in BRB80 buffer (80 mM Pipes, 2 mM $MgCl_2$ and 1 mM EGTA), transferred to a coverslip and covered with halocarbon oil after the removal of the excess buffer. Yolk autofluorescence was excited by a 405 nm CO_2 laser beam and detected in the 425-475 nm spectrum in an Olympus FV1000 confocal microscope.

Confocal reflection microscopy (CRM) and image analysis were carried out according to Gaspar and Szabad (Gaspar and Szabad, 2009). Briefly, for reflection imaging the 633 nm He-Ne laser line with 0.6-1.0 mW power was used in combination with an LP560 emission filter and the third-in-order photomultiplier. Such arrangement allows simultaneous combination of CRM with fluorescence imaging. There were 19.5-second long high-speed recordings (~15 f.p.s., a total of 300 frames) conducted over 20.9×20.9 μm^2 cytoplasm areas, two for every analyzed early stage 12 oocyte, which were selected randomly. The recordings were analyzed for the lipid-droplet motion direction and speed, other than the ooplasmic streaming. Movement of the lipid droplets was tracked by using the SpotTracker plug-in of ImageJ (http://rsb.info.nih.gov/ij/). Analysis of the trackings was done by a series of custom-made Excel macros in order to split the trackings to individual runs and pauses.

Statistical analysis of the data was carried out using SPSS 15. One-way ANOVA tests were used for comparison of the means. Pair-wise Kaplan-Meier tests and the Cox regression analysis was used for survival analysis of lipid droplet runs. The MSD plot, as described in the text, and the curve fittings were done in Microsoft Excel.

The authors thank the reviewers for their helpful comments on the first version of the manuscript. Support for the work came from a grant from the Hungarian Scientific Research Fund (OTKA NI69180) and from the Graduate Student Program of the University of Szeged.

References

Cross, R. A. (2004). The kinetic mechanism of kinesin. *Trends Biochem. Sci.* **29**, 301-309.

Cytrynbaum, E. N., Scholey, J. M. and Mogilner, A. (2003). A force balance model of early spindle pole separation in Drosophila embryos. *Biophys. J.* **84**, 757-769.

DeRenzo, C. and Seydoux, G. (2004). A clean start: degradation of maternal proteins at the oocyte-to-embryo transition. *Trends Cell Biol.* **14**, 420-426.

Erdelyi, M. and Szabad, J. (1989). Isolation and characterization of dominant female sterile mutations of Drosophila melanogaster. I. Mutations on the third chromosome. *Genetics* **122**, 111-127.

Foe, V. E., Odell, G. M. and Edgar, B. A. (1993). Mitosis and morphogenesis in the Drosophila embryo: point and counterpoint. In *The Development of Drosophila melanogaster* (ed. M. Bate and A. Martinez Arias), pp. 149-300. Cold Spring Harbor, NY: Cold Spring Harbor Laboratory Press.

Gaspar, I. and Szabad, J. (2009). *In vivo* analysis of MT-based vesicle transport by confocal reflection microscopy. *Cell Motil. Cytoskeleton* **66**, 68-79.

Gepner, J., Li, M., Ludmann, S., Kortas, C., Boylan, K., Iyadurai, S. J., McGrail, M. and Hays, T. S. (1996). Cytoplasmic dynein function is essential in Drosophila melanogaster. *Genetics* **142**, 865-878.

Ghosh-Roy, A., Kulkarni, M., Kumar, V., Shirolikar, S. and Ray, K. (2004). Cytoplasmic dynein-dynactin complex is required for spermatid growth but not axoneme assembly in Drosophila. *Mol. Biol. Cell* **15**, 2470-2483.

Gross, S. P., Welte, M. A., Block, S. M. and Wieschaus, E. F. (2000). Dynein-mediated cargo transport *in vivo*. A switch controls travel distance. *J. Cell Biol.* **148**, 945-956.

Hoenger, A., Sack, S., Thormahlen, M., Marx, A., Muller, J., Gross, H. and Mandelkow, E. (1998). Image reconstructions of microtubules decorated with monomeric and dimeric kinesins: comparison with x-ray structure and implications for motility. *J. Cell Biol.* **141**, 419-430.

Kalfayan, L. and Wensink, P. C. (1982). Developmental regulation of Drosophila alpha-tubulin genes. *Cell* **29**, 91-98.

Kalfayan, L., Loewenberg, J. and Wensink, P. C. (1982). Drosophilia alpha-tubulin genes and their transcription patterns. *Cold Spring Harb. Symp. Quant. Biol.* **46**, 185-190.

Karpova, N., Bobinnec, Y., Fouix, S., Huitorel, P. and Debec, A. (2006). Jupiter, a new Drosophila protein associated with microtubules. *Cell Motil. Cytoskeleton* **63**, 301-312.

Kikkawa, M. and Hirokawa, N. (2006). High-resolution cryo-EM maps show the nucleotide binding pocket of KIF1A in open and closed conformations. *EMBO J.* **25**, 4187-4194.

Klumpp, L. M., Brendza, K. M., Rosenberg, J. M., Hoenger, A. and Gilbert, S. P. (2003). Motor domain mutation traps kinesin as a microtubule rigor complex. *Biochemistry* **42**, 2595-2606.

Lakamper, S. and Meyhofer, E. (2005). The E-hook of tubulin interacts with kinesin's head to increase processivity and speed. *Biophys. J.* **89**, 3223-3234.

Marx, A., Muller, J., Mandelkow, E. M., Hoenger, A. and Mandelkow, E. (2006). Interaction of kinesin motors, microtubules, and MAPs. *J. Muscle Res. Cell Motil.* **27**, 125-137.

Mathe, E., Boros, I., Josvay, K., Li, K., Puro, J., Kaufman, T. C. and Szabad, J. (1998). The Tomaj mutant alleles of alpha Tubulin67C reveal a requirement for the encoded maternal specific tubulin isoform in the sperm aster, the cleavage spindle apparatus and neurogenesis during embryonic development in Drosophila. *J. Cell Sci.* **111**, 887-896.

Matthews, K. A., Miller, D. F. and Kaufman, T. C. (1989). Developmental distribution of RNA and protein products of the Drosophila alpha-tubulin gene family. *Dev. Biol.* **132**, 45-61.

Matthews, K. A., Rees, D. and Kaufman, T. C. (1993). A functionally specialized alpha-tubulin is required for oocyte meiosis and cleavage mitoses in Drosophila. *Development* **117**, 977-991.

Matthies, H. J., Messina, L. G., Namba, R., Greer, K. J., Walker, M. Y. and Hawley, R. S. (1999). Mutations in the alpha-tubulin 67C gene specifically impair achiasmate segregation in Drosophila melanogaster. *J. Cell Biol.* **147**, 1137-1144.

Mizuno, N., Toba, S., Edamatsu, M., Watai-Nishii, J., Hirokawa, N., Toyoshima, Y. Y. and Kikkawa, M. (2004). Dynein and kinesin share an overlapping microtubule-binding site. *EMBO J.* **23**, 2459-2467.

Paddock, S. (2002). Confocal reflection microscopy: the "other" confocal mode. *Biotechniques* **32**, 274, 276-278.

Palacios, I. M. and St Johnston, D. (2002). Kinesin light chain-independent function of the Kinesin heavy chain in cytoplasmic streaming and posterior localisation in the Drosophila oocyte. *Development* **129**, 5473-5485.

Saxton, W. M., Hicks, J., Goldstein, L. S. and Raff, E. C. (1991). Kinesin heavy chain is essential for viability and neuromuscular functions in Drosophila, but mutants show no defects in mitosis. *Cell* **64**, 1093-1102.

Schief, W. R. and Howard, J. (2001). Conformational changes during kinesin motility. *Curr. Opin. Cell Biol.* **13**, 19-28.

Schief, W. R., Clark, R. H., Crevenna, A. H. and Howard, J. (2004). Inhibition of kinesin motility by ADP and phosphate supports a hand-over-hand mechanism. *Proc. Natl. Acad. Sci. USA* **101**, 1183-1188.

Serbus, L. R., Cha, B. J., Theurkauf, W. E. and Saxton, W. M. (2005). Dynein and the actin cytoskeleton control kinesin-driven cytoplasmic streaming in *Drosophila* oocytes. *Development* **132**, 3743-3752.

Sharp, D. J., Rogers, G. C. and Scholey, J. M. (2000). Microtubule motors in mitosis. *Nature* **407**, 41-47.

Shubeita, G. T., Tran, S. L., Xu, J., Vershinin, M., Cermelli, S., Cotton, S. L., Welte, M. A. and Gross, S. P. (2008). Consequences of motor copy number on the intracellular transport of kinesin-1-driven lipid droplets. *Cell* **135**, 1098-1107.

Szabad, J., Erdélyi, M., Hoffmann, G., Szidonya, J. and Wright, T. R. (1989). Isolation and characterization of dominant female sterile mutations of *Drosophila melanogaster*. II. Mutations on the second chromosome. *Genetics* **122**, 823-835.

Tadros, W. and Lipshitz, H. D. (2005). Setting the stage for development: mRNA translation and stability during oocyte maturation and egg activation in Drosophila. *Dev. Dyn.* **232**, 593-608.

Theurkauf, W. E. (1992). Behavior of structurally divergent alpha-tubulin isotypes during Drosophila embryogenesis: evidence for post-translational regulation of isotype abundance. *Dev. Biol.* **154**, 205-217.

Uchimura, S., Oguchi, Y., Katsuki, M., Usui, T., Osada, H., Nikawa, J., Ishiwata, S. and Muto, E. (2006). Identification of a strong binding site for kinesin on the microtubule using mutant analysis of tubulin. *EMBO J.* **25**, 5932-5941.

Venkei, Z. and Szabad, J. (2005). The Kavar(D) dominant female-sterile mutations of Drosophila reveal a role for the maternally provided alpha-tubulin4 isoform in cleavage spindle maintenance and elongation. *Mol. Genet. Genomics* **273**, 283-289.

Venkei, Z., Gaspar, I., Toth, G. and Szabad, J. (2006). alpha4-Tubulin is involved in rapid formation of long microtubules to push apart the daughter centrosomes during earlyx *Drosophila* embryogenesis. *J. Cell Sci.* **119**, 3238-3248.

Vesely, P. and Boyde, A. (2001). Fast intracellular motion in the living cell by video rate reflection confocal laser scanning microscopy. *J. Anat.* **198**, 641-649.

Wang, Z. and Sheetz, M. P. (2000). The C-terminus of tubulin increases cytoplasmic dynein and kinesin processivity. *Biophys. J.* **78**, 1955-1964.

Welte, M. A. (2007). Proteins under new management: lipid droplets deliver. *Trends Cell Biol.* **17**, 363-369.

Welte, M. A., Gross, S. P., Postner, M., Block, S. M. and Wieschaus, E. F. (1998). Developmental regulation of vesicle transport in Drosophila embryos: forces and kinetics. *Cell* **92**, 547-557.

Woehlke, G., Ruby, A. K., Hart, C. L., Ly, B., Hom-Booher, N. and Vale, R. D. (1997). Microtubule interaction site of the kinesin motor. *Cell* **90**, 207-216.

Yamamoto, A. H., Komma, D. J., Shaffer, C. D., Pirrotta, V. and Endow, S. A. (1989). The claret locus in Drosophila encodes products required for eyecolor and for meiotic chromosome segregation. *EMBO J.* **8**, 3543-3552.

Yonekura, H., Nomura, A., Ozawa, H., Tatsu, Y., Yumoto, N. and Uyeda, T. Q. (2006). Mechanism of tail-mediated inhibition of kinesin activities studied using synthetic peptides. *Biochem. Biophys. Res. Commun.* **343**, 420-427.

Yun, M., Bronner, C. E., Park, C. G., Cha, S. S., Park, H. W. and Endow, S. A. (2003). Rotation of the stalk/neck and one head in a new crystal structure of the kinesin motor protein, Ncd. *EMBO J.* **22**, 5382-5389.